

Quality Assurance Studies of Publicly Desirable Nepal Made PPC Cements via the Instrumental Characterization Methods

Prof. Dr. Anant Babu Marahatta^{1,*}, Puspa Kamal Dahal²

¹Supervisor/Professor of Chemistry, Engineering Chemistry and Applied Science Research Unit, Departments of Civil, Computer & Electronics Communication & Information Engineering, Kathford Int'l College of Engineering and Management (Affiliated to Tribhuvan University), Kathford Int'l Education & Research Foundation, Kathmandu, Nepal

²Student, Department of Civil Engineering, Kathford Int'l College of Engineering and Management (Affiliated to Tribhuvan University), Kathford Int'l Education & Research Foundation, Kathmandu, Nepal

*Corresponding author: abmarahatta@gmail.com/anant.marahatta@kathford.edu.np



Abstract – The PPC cements and their ultra-fine grainy matrix are widely recognized as ideal engineering materials due to their unique cementitious features owing to dispense exceptional placing, adhering, setting, and enduring abilities. The underlying key parameters deterministic to all these distinctive potentialities are quality of the pozzolana, type of the crystallite phases & their average size distributions, and the particular identities of the chemical moieties/functional groups. The precise assessments of each of them instrumentally in variable technology manufactured yet publicly desirable ready-to-use dry PPC cements always provide the trustworthy means of granting not only their entire qualities but also unequal aptitudes for workability, compressive strength, stability of the C–S–H (I) & C–S–H (II) gluing gels, water penetration & permeability resilience, sustainability of the concrete structures, hair cracking preventions, etc. In this study, we employed XRD and FTIR spectroscopic techniques, and characterized all the founding chemical phases needful to assure the quality of the four topmost PPC cements branded across the commercial markets of Nepal. The critical spectral interpretations of the: (a) diffractograms reveal alite, belite, & silicates as predominant; portlandite, & calcite as premier; fly ash, gypsum, aragonite, & vaterite as subsidiary; and silica, arsenate, & organic traces as ultra-trace crystallite phases; and (b) IR spectrograms verify all the chemical fragments and functional groups of each of these phases such as Ca–O (fly ash); Si–O–Si (silica, α -quartz); S–O of SO_4^{2-} (gypsum (CaSO_4)); CO_3^{2-} of CaCO_3 polymorphs; As–O of AsO_4^{3-} (calcium arsenates); Si–O of alite (Ca_3SiO_5) & belite (Ca_2SiO_4); SiO_4^{4-} & SiO_4^{2-} of silicate tetrahedra & polymerized orthosilica ($\text{Si}_2\text{O}_7^{6-}$); O–H & H–O–H of hydrous portlandite & crystal water of the calcite and gypsum; C–H of organic traces; and O–H of granularly adsorbed/absorbed molecular water (H_2O) & H-bound OH (H–OH) segments. We strongly believe that this research article illuminates the standard measures of assessing real quality of the PPC cements and of standardizing their Nepal Standard (NS) codes.

KEYWORDS – PPC cement, Grain morphology, Health hazards, Alite/Belite/Calcite/Gypsum.

1. INTRODUCTION

In the engineering constructions, various types of the cements such as ordinary Portland cement (hereafter, OPC), Portland Pozzolana cement (hereafter, PPC), Portland slag cement (hereafter, PSC) etc., are massively used as the most fundamental cornerstone worldwide dispensing exceptional gluing, placing, stiffening, adhering, hardening, and enduring potentialities with consecutive hydration reactions with water. These characteristic features are mostly governed not only by their unique particle morphology such as crystallite

sizes, grain/particle sizes, low to moderate range particle size distributions, relatively high specific surface area with good degree of porosity, etc., but also diversified yet comprehensive hydration reaction products acquired by them in wide range applicative composite materials (low to high strength cement-pastes, mortars, plasters, concretes and reinforced concretes, etc.). Additionally, the wide range porosity networks, dissimilarly constituted crystallite chemical phases, low to high degree of denseness, better workability with significant slump value, higher compressive strength even in the shorter setting time regimes, remarkable evaporable water (absorbed & capillary water) holding/retaining capillaries, etc. surpass their cementitious features significantly [1–6]. Few of the supporting evidences standing firmly on behalf of all those captivating characteristic features of the cements owing to the excessive demands of them universally is remarkably high consumption trends (4 bMt/year (billion metric ton)), excessive production rates (top three countries: China–58.1%, India – 6.7%, US–2%), and immense CO₂ emission records (second in rank, (5–8 % of total human-induced CO₂ emission, and 2.08 Gt (gigaton) in amount globally)) [1]. Even in the context of developing countries like Nepal, the concerned quantitative values associated with the nationwide consumptions and commercial market demanding rates of the different grades cements are also very promising: the latest annual per capita cement consumption rate is 303 kg (India; 195 kg, China; 1,716 kg, Bhutan; 734 kg) [7], per capita CO₂ emission is 0.12mMt (million metric ton) in 2019 (total contribution = 0.06% of the global emission (China: 15%, US: 2%, Germany: 2.9%) [1(b)], India = 164mMt), and the net demand rate forecasted for the fiscal year 2024–2025 is 26 million tons/year. More particularly in Nepal, the (a) total capacity of cement productions, net integrative manufactures, and bulk demands nationwide are 15 mMt/year, 7.49 mMt/year, and 9.05 mMt/year respectively; (b) total quantity of cement production rate per day is 4,225 tons (foreign investment factories: 2,783 tons, state-owned factories: 820 tons, and privately run factories: 622 tons); (c) net investments injected by the foreign and Nepali citizens are of market values \$0.43 billion, and \$0.92 billion US respectively; (d) net quantity of limestones utilized by the foreign and state-owned factories for producing 1 ton of cement are 0.99 tons and 1.45 tons in average respectively; (e) total number of registered, operational, and nonoperational cement plants are 124, 66, and 58 respectively [1(b)]; (f) total amount of clinkers consumed per year is around 7 mt/year [7, 8]; (g) importing and exporting frequencies attain the figures 123rd largest importer in the world [9] but relatively lower exporter (Nepalese cements worth around \$0.02 billion US are exported in the fiscal year 2023–2024 to India (\$5.85 million US in 2022–2023 [10]); and (h) per capita GDP (1987/1988–2019/2020) and human development index (HDI) (1990–2019) associated with the cement productions are $p < 0.01$; $R^2 = 0.90$ and $p < 0.01$; $R^2 = 0.84$ respectively [1(b)]. Based on all these prevailing market economies and dynamics plus the rapid momentums gained by the cement industries across the country, we can speculate that Nepal hosts technologically modernized, functionally potent, operationally viable, productionally diverse, and brandwise quite standard cements of different types. However, it still needs to adopt various state-of-the-art cement production technologies, install the additional industrial plants, operate the existing plants in a full-fledged condition, functionalize the local clinker productions, regularize the clinker supply from the foreign lands, etc. in order to meet the nationwide demand-supply chains of the good quality/grades cements plus to ensure their sudden market shortage. Towards the same, few major initiatives taken by the Nepalese governments such as (a)

accelerating the production rates of OPC, PPC, and PSC type cements with the effective implementations of the ISO grading systems (minimum grade: 33, and high-quality grades: 43 & 53), (b) encouraging the local clinker productions and preservations of the locally available raw materials and mine areas, (c) launching the national integrated clinker production plants, (d) regularizing the timely supply of the standard ingredients, and the associated raw materials of the clinkers, (e) welcoming the foreign investments and operating them under dynamic Nepal Standard (NS) code, (f) establishing the road networks across the mining areas, clinker factories, and cement industries, etc., [11–14] have boosted up the entire performance of the industrial plants.

Despite all those motivating practical efforts of improvising the standards of the Nepal made cements and of strict implementations of the NS standard quality assurance throughout the production plants & the national-mega construction projects, the commercial markets of Nepal are still looking for the high standard cements offering good cementitious features and enduring abilities in order to fulfill the nationwide desires and public demands. Alike to this, people around the nation are also questioning the quality of the national and international cements branded across Nepal, and are still reluctant to use them properly with good confidence and satisfactory assurance. In the course of attempting the questionable qualities of all the cements and cement based products prevailing mostly in the ongoing mega construction projects and general commercial markets of Nepal, present author first-ever addressed many key aspects of them by characterizing the publicly desirable yet top ranked cement industry produced ready-to-use OPC cement powders and their time dependent hydration reaction products acquired by them in the specific mortars explicitly with potential instrumental methods (X-ray diffraction and Fourier Transform Infra-Red spectroscopies), and thereafter theorized their chemical compositions herewith [13, 15] wherein the most probable contributions of every chemical constituents towards achieving promising placing, adhering, setting, hardening, and enduring propensities as a function of hydration reactions time are disclosed, and underscored the primary requisites needful for standardizing the quality of the cements and for meeting their specific NS code. Therewith, we excluded the Nepal made PPC brands as the experimental specimens even though they are: (a) major stakeholders of the various ongoing national pride construction projects and ranked first in reference to gross cement productions by mass in Nepal (OPC: 40%, PPC: 50%, PSC: 10% [1(b)]), (b) environmentally friendly, technologically low cost, construction wise cheaper, and environmental CO₂ emission wise better, (c) hydraulic blended cement comprising with the low percentage clinker but high percentage pozzolana (PPC: 65% clinker, 5% gypsum, and 30% pozzolana; OPC: 95% clinker and 5% gypsum) [6,12,1(b)], (d) high strength and better physical & mechanical properties dispensing cements with good workability (less risks of hair cracking, more durability, and sustainability), more uniform surfaces on casting materials, and recognizable enduring abilities (resistant to the sulfate/chloride attacks) even in the aggressive environmental and underwater conditions [6], (e) more finely grained cement with considerable hydration affinities: the secondary hydration reactions products (silicate gel (C–S–H (II)) of the pozzolana offer higher reinforcing potentiality than that of the C–S–H (I) released priory from those type chemical constituents that are as similar as in OPC), (f) general construction cements with low heat of hydration, less attentions required for the post-treatment/curing, and comparable setting time, thermal expansion/ contraction & compressive strength to that of the OPC, etc., [6,16]. Herewith, we stressfully carried out the similar type spectroscopic studies on

preferentially selected yet variable technology (domestic and foreign run industries) manufactured commercially desirable ready-to-use PPC cement powders, and characterized their distinctive crystallites/grain/particle morphology, explicit chemical phases, key chemical constituents/fragments/formulations, etc., along with the genuine predictions of the average particle size distribution ranges, most probable hydration propensities and temporal chemical kinetics, evaporable water retaining/holding abilities, most potential chemical constituents quantitatively, and their utmost contributions towards exhibiting remarkable working aptitudes. To the knowledge of the present authors, no research works concentrating fully on such type instrumental characterizations & quantitative estimations of the in-built functional chemical constituents, and the most potential means of quality assurance studies of the Nepal made PPC brand cements are available. Instead, very qualitative judgements and nominal ways of assessing their performances in mortar and concrete mixtures are reported elsewhere [1, 6, 11, 12, 14, 17], wherein the descriptors such as degree of fineness, setting time, compressibility, thermal expansion /contraction, enflamed CO₂ emissions, nationwide/localized consumption and demand trends, gross industrial energy consumptions, etc. are undertaken while accounting workability of the specific brand PPC cement/s. In the light of all these circumstances, this quantitative research work serves as standalone enclosures of all the requisites required for assuring their qualities such as standardizing the clinker phases and the locally available raw materials, improvising the industrial technologies and production strategies, modernizing the production plants, implementing the effective health, safety, and prevention policies, maximizing the industrial and academic R & D, updating the national PPC-cement manufacturing guidelines and NS codes, and maintaining the overall production norms associated with them. The entire article is structured as: Materials & Methods in section 2, Results & Discussions in section 3, and Summary & Conclusions in section 4.

2. MATERIALS AND METHODS

2.1 Collection of the PPC Cements

We collected the required amounts of the four preferentially selected variable technology manufactured dry ready-to-use PPC cement in powdered forms directly from the Kathmandu (Nepal) based cement depots owned by the manufacturers, viz.; Hongshi, Brij, United, and Sarbottam where the large quantities of them are stored in the high-density polyethylene made 50 kg sacs, and are dispatched to the construction sites as per the orders of the consumers. Actually, the depots are constructed in the elevated areas where the internal degrees of humidity, dampness, and temperature are maintained in their favor, and the cement sacs stacked one over the other are fully partitioned using waterproof polymeric sheets. In order to maintain the confidentialities of the manufacturers, and to skip the most possible conflict of interests existing in their products branded across Nepal, all the cement samples were named as AP1, AP2, AP3, and AP4 without any prior orders, designated with the same throughout this study. The equal attentions were also given to their explicit industrial R & D characteristic features disclosed to the public, and the overall industrial cement production strategies nationwide. In collecting every sample specimens, the separate polyethylene bottles with air tight stoppers were used, and the aluminum foil was layered internally just to prevent the cement powders from the direct exposures of the humid weather as shown in Figure 1. Throughout all the sampling procedures, the characteristic physicochemical properties of the every cement brands were securely preserved, and

remained intact fully from the effects of heat and temperature, moisture and humidity, mold and dampness, squeezed and pressurized destroying, etc. Accordingly, the (a) most probable chemical constituents, (b) compressive/enduring strengths, and hydration reactions propensities, (c) manufacturing technologies with ecofriendly procedures, (d) pre- & post- treatment attentions, (e) quality of the clinker and raw materials employed, and (f) popularity and market dynamics across the Kathmandu valley, etc. of them were also considered genuinely.

2.2 Measurements of the X-ray Diffractograms

For the specific XRD measurements, the four preferentially selected powdered cement samples (AP1, AP2, AP3, and AP4) of four different commercial brands were submitted to Nepal Academy of Science and Technology (NAST); a government owned research organization offering an XRD facility to the academia and industrial sectors for very nominal service charge. At the time of submission, all the cement samples were fully sealed in separate polyethylene bottles with aluminum layered stoppers (Figure 1), and were strictly asked to unseal them turn by turn at the time of injecting them into the sample compartment of the XRD diffractometer. The diffractometer offered therewith for the spectroscopic measurements was BRUKER D2 PHASER; a bench-top instrument equipped with the unique detector and digital monochromator mode for unwanted sample florescence and background scattering, and can deliver relatively high quality data with rapid assembling rates. While measuring the XRD spectral patterns in 2θ angular range of $10-90^\circ$, a step size of an angular increment 0.02° , and a material scanning rate of $0.5^\circ/\text{min}$ was adjusted instrumentally. And, for the subsequent XRD spectral analyses and interpretations, the concerned raw datasets of each sample specimen were plotted as diffractogram where the number of counts and 2θ (coupled two theta/theta) values are scaled on the Y- and X- axis respectively.

2.3 Measurements of the Fourier Transform Infrared (FTIR) Spectrograms



Figure 1. Four different sample holders (polyethylene bottles) containing experimental specimens of AP1, AP2, AP3, and AP4 cements are securely stoppered with aluminum foil layers internally.

Alike to the XRD measurements, the four variable technology manufactured PPC cement samples (AP1, AP2, AP3, and AP4) were submitted to NAST for the Fourier Transform Infrared (FTIR) spectroscopy measurements. As shown in Figure 1, all these four analyte specimens were fully sealed in polyethylene bottles with aluminum layered stoppers, and were asked to unseal them turn by turn at the time of preparing their pellets with KBr powder (a sample carrier offering an optically transparent feature within the IR frequency range of the FTIR spectrophotometer). The entire spectroscopic measurements was carried out with 'Shimadzu IR Tracer-100'; a high precision equipment inbuilt with outstanding measurement speed, sample sensitivity, and spectral resolutions with easy-to-use analytical software. Prior to measuring the IR spectra, the spectrophotometer was calibrated at ambient air conditions, and its internal functions were made standardized. In every measurements, a small KBr-pellet of the every cement samples was fed, and the concerned interferogram was recorded within the instrumental range of absorption frequency ($400\text{--}4000\text{ cm}^{-1}$), resolution limit (4 cm^{-1}), and sample scanning rate (50/sample). The Fourier transformation technique was employed while converting the concerned interferograms into the easy-to-interpret IR spectra.

2.4 XRD–Peak Fittings with *Gaussian* Convolution

In order to find out the interatomic-layer distance (d), average crystallite- (L), grain-, and particle- sizes of all the four PPC cement samples, we at first identified the most intense XRD peak of each of them at the specific diffraction angle ($2\theta_{max}$), and retrieved the required datasets (intensity vs peripheral angles (2θ) of $2\theta_{max}$) explicitly. Each dataset of each sample specimen was spreaded with Microsoft Excel spreadsheet, and was simulated lively with the *Gaussian* convolution. Prior to this, the specific Cartesian coordinates essential for sketching the *Gaussian* convolution in a 3D space were programmatically created in the same spreadsheet, and the required parametric standardizations was carried out as per the needs of optimum peak-fitting techniques. In the course of the same, the specific values of the controlling parameters such as peak height (H), peak width (W), and full-width at half-maximum (herewith, FWHM (β)) were determined followed by the accurate estimations of the net integral areas (mm^2) $\{A = \frac{H \times \beta}{0.3989 \times 2.35}\}$ lying under every predominant bands of the samples. The diffraction angle θ assigned to the intense spectral bands of every cement sample was substituted in Bragg's equation (Eq. 1), and the interatomic-layer distance d (basal spacing) was computed.

$$n\lambda = 2d \sin(\theta) \quad (1)$$

Where;

n = order of diffraction.

λ = wavelength of the incident X-ray ($\lambda = 1.54\text{ \AA}$)

θ = angle of incidence

And, thus computed FWHM value (β) of the most intense peak only of every samples was used to determine the crystallite size L of their predominant phases by employing Scherrer's formula (Eq. 2).

$$L = (K \times \lambda) / (\beta \times \cos(\theta)) \quad (2)$$

Where;

K = Scherrer's constant.

The numeral value for the constant K was derived by using the relation formulated in Eq. 3; a formula recommended for those cases where the (a) FWHM value is determined through the *Gaussian* peak fitting technique, and (b) material to be investigated contains maximum percentage spherical particulates (the PPC cements are manufactured with optimum proportions of the 'fly ash') [5, 6].

$$K = 2\sqrt{(\ln 2)/\pi} \cong 0.9394 \quad [18, 19] \quad (3)$$

Each specific values of L and d of every samples were substituted in Eq. 4, and the number of parallel interatomic planes m of their predominant crystallite phases were determined.

$$m = \frac{L}{d} \quad (4)$$

3. RESULTS AND DISCUSSIONS

3.1 Physicochemical Properties of PPC Cements

Alike to the wide range chemical compositions of the Nepal made OPC cements [13], the PPC brands may contain more varieties yet relatively rigorous type chemical constituents owing to furnish an exceptional workability more especially in such type of engineering constructions where the performances of the OPC are recognizably poor. Some of the sound engineering and technological practices where the engineers, contractors, consultants, builders, owners, etc. preferably employ PPC type cements are (a) water permeability and $\text{Ca}(\text{OH})_2$ leaching resistance in high density concrete materials, (b) enduring improvement of the mortar mixtures and concretes with the betterment in shrinkage, and thermal expansions/contractions, (c) hair-cracking reduction/ prevention on the concrete made structures, (d) hydration reactions kinetics enhancement with good quality chemical products, (e) heat of hydrations decrement and the sudden cracking lowering, (f) discarding of the additives such as plasticizer, silica cement, high alumina cement, etc. for strengthening the structures, (g) retarding corrosive attacks to the reinforced bars and annealed wires (masonry structures), (h) acquiring higher passivity, compactness, flexural tensile strength, and durability even in the aggressive environmental attacks (acid rain, salty/alkaline/ mineral water, mineralized soil/clay, chloride/sulfate/hydroxide enriched aqueous media, etc.), etc. [14–16, 20, 21]. The uniqueness of the PPC cements towards offering all those privileges and granting the significant values to all those accountable descriptors lie basically in their fundamental ingredients and raw materials plus quite contrasting formulations/foundations to that articulated for the OPC cements. In fact, the PPC is a blended type cement manufactured by intermixing clinker particles with the pozzolanic materials (5–25% by weight) and binary chemical compounds (slag, and gypsum); or sometimes by directly blending OPC cements with the required amount of the fly ash (CaO) and slag. And, the most common sources from where the artificial and natural Pozzolana materials are extracted (Pozzolana attributes to pozzolanic features including placing and setting

abilities, hardening and enduring potentialities, etc.) are burnt- clay/shale/maize/rice husks/diatom shells & smectite clay (moler), calcined clay; and the direct deposits erupted from the active volcanos respectively [6, 12, 20]. The same granular and core level dissimilarities in the wide range particulates materials and functional units holding chemical phases of the PPC act as the actual bases of acquiring relatively more promising type hydration reactions products than that of the OPC [15–20]. And, they are the premier chemical compounds that exhibit comprehensive responsibilities towards bestowing marvelous setting, hardening, and enduring potentialities to the PPC cement made engineering structures and designs. According to the hydration reactions trends and time dependent chemical reaction mechanisms studies of the blended cements, and the SEM, IR, and XRD based instrumental characterizations reported elsewhere [22–24], the PPC generates two types silicate hydrate gels, viz., C–S–H (I) and C–S–H (II) as hydration reaction products through the subsequent primary and secondary type reactions upon the continuous curing/ treatment with water. The first product is produced by reacting the silicates $2\text{CaO}.\text{SiO}_2$ or Ca_2SiO_4 (belite, C_2S) & $3\text{CaO}.\text{SiO}_2$ or Ca_3SiO_5 (alite, C_3S); plus the aluminates $3\text{CaO}.\text{Al}_2\text{O}_3$ or $\text{Ca}_3\text{Al}_2\text{O}_6$ (C_3A) of the clinker phases with water ($\text{Clinker} + \text{Water} \rightarrow \text{C–S–H (I)} + \text{Ca(OH)}_2$) just like in OPC cement; but the second product is derived uniquely from the reaction between thus released Ca(OH)_2 and Pozzolana ($\text{Ca(OH)}_2 + \text{Fly Ash/Slag} \rightarrow \text{C–S–H (II)}$). And, in terms of the functions of the C–S–H gel in strengthening entire concrete structures, and in enduring them in multiple aspects, the lately derived yet PPC only acquired C–S–H (II) matrix is ranked superior. In fact, the concrete structures gained by the cements are the progressively evolved motifs from the very early stage (cement-sand-pebbles-water paste) by passing through the series of the steps each experiencing contrasting developments in the physicochemical properties, viz., placing (plastic), adhering, setting (stiffening), hardening, & enduring; and the net succeeding hydration reactions occurred with water as a function of time at ambient temperature regimes are the principal driving forces towards fixing the composite materials in definite shapes and sizes. The more important yet predominantly associated consequences are underlying with the direct dependencies of the hydration reaction propensities, types of the hydration reaction products, and the entire quality of the C–S–H gel matrices on crystallite sizes, granular distribution ranges, types of the crystallite phases, quality of the clinkers, clinker phases and raw materials, porosity networks and specific surface areas, amounts of the chemical constituents and functional groups, etc. of the cements. The most potential instrumental means through which we can assess all these granular descriptors quantitatively, and assure the quality of all type cement products are XRD and FTIR spectroscopies [13, 15]. In this research report, we instrumentally reveal all those contributing attributes responsible for assuring the quality of the variable technology produced dry ready-to-use PPC cements available in the commercial markets of Nepal.

3.2 Interpretations of the XRD Diffractograms

The powder XRD instrumental technique and the associated diffraction pattern analyses are not new to the fields where proper characterizations of the engineering materials are assessed quantitatively. As this technique offers materials scanning facility nondestructively with the explicit usages of the monochromatic X-ray radiation of the wave length $\lambda = 1.54 \text{ \AA}$, and dispenses the unique type diffraction spectra for the unique configurations of the crystallite phases of the materials, the frequent employment of it worldwide for the

quality assurance studies of the variable technology derived ready-to-use multifaceted cements and their composites with the exclusive reveals of their grain morphology and founding chemical phases is genuine [4, 13, 15, 16]. Since the cements and cement made consumable products are classified as ideal materials because of the granular integration of the nanometer sized crystallites made up of characteristic clinker phases with the exclusive stacking of the interatomic layers separated by the distance d , and the most distinguished hydration reactions products with water, the XRD patterns diffracted by their founding clinker phases at unidentical diffraction angles (2θ) would be the most imperative means of forecasting their workability and granular compositions. In this research work, we probed the same core-level identities apparent to the PPC brand cements, and assured the quality of them in reference to the Nepal made products AP1, AP2, AP3, and AP4 (Figure 1).

The concerned X-ray diffraction patterns of the AP1, AP2, AP3, and AP4 are displayed in Figure 2 and Figure 3 respectively, wherein the most intense spectral peak of each sample is marked with the specific diffraction angle ($2\theta^0$). The angular value in which the relatively low counts/less intense peaks are raised are not highlighted as they contribute less towards speculating the predominant size of the crystallites, thickness, and the most probable range of the particulate size distributions. The respective fingerprint angular regions ($2\theta_{max}$) indicative to the predominant crystallite phases of the AP1, AP2, AP3, and AP4 cement brands in which the most intense spectral bands are appeared are 26.920° , 29.893° , 27.149° , and 26.920° respectively. The net integral area (A) under these bands are estimated as 604 mm^2 , 315 mm^2 , 595 mm^2 , and 392 mm^2 respectively (Figure 4 and Figure 5). These angles are comparatively smaller than the angle $2\theta = 33^\circ$, a fingerprint diffraction angle of the CaCO_3 (calcite) phases (one of the most significant clinker phases that remains persistent from the very preliminary manufacturing stages of the cements) and gypsum (CaSO_4). In particular, the appearance of the most intense spectral peaks with dissimilar magnitudes of the peak area for the AP1, AP4, and AP3 samples at $2\theta_{max} \approx 26.920^\circ$ (AP1: $A = 604 \text{ mm}^2$, AP4: $A = 392 \text{ mm}^2$) and 27.149° ($A = 595 \text{ mm}^2$) respectively signify the absolute presence of the portlandite ($\text{Ca}(\text{OH})_2$), alite ($3\text{CaO} \cdot \text{SiO}_2$ or Ca_3SiO_5), aragonite, and vaterite ($2\theta_{max} \approx 27.02^\circ$) (CaCO_3 has three polymorphs: calcite, aragonite, and vaterite) phases in them; and the similar type peak, but standing at $2\theta_{max} = 29.893^\circ$ for the AP2 ($A = 315 \text{ mm}^2$) sample corresponds to the cumulative combinational diffraction effects caused by the gypsum, alite, and calcite phases. Area wise approximations, the quantitative amount of the predominant alite phases present in the four PPC sample specimens would be $\text{AP1} > \text{AP3} > \text{AP4} > \text{AP2}$. Prior to utilizing all those $\theta_{max} = 2\theta_{max}/2$ values in finding out the interlayer distance d (Bragg's law) between any two successive atomic-planes of the predominant crystallite phases of each sample specimen, their crystallite sizes (L) and thickness (Scherrer's formula), and the total number of parallel atomic-planes (m) stacked one over the other, we have at first characterized all the remaining yet relatively less prominent XRD bands (Figure 6). The very first band appeared at $2\theta \approx 21^\circ$ (specific to the alite phases) for the samples AP1, AP3, and AP4 genuinely supports their own $2\theta_{max}$ diffraction angle, and justifies that the alite is one of their most predominant crystallite

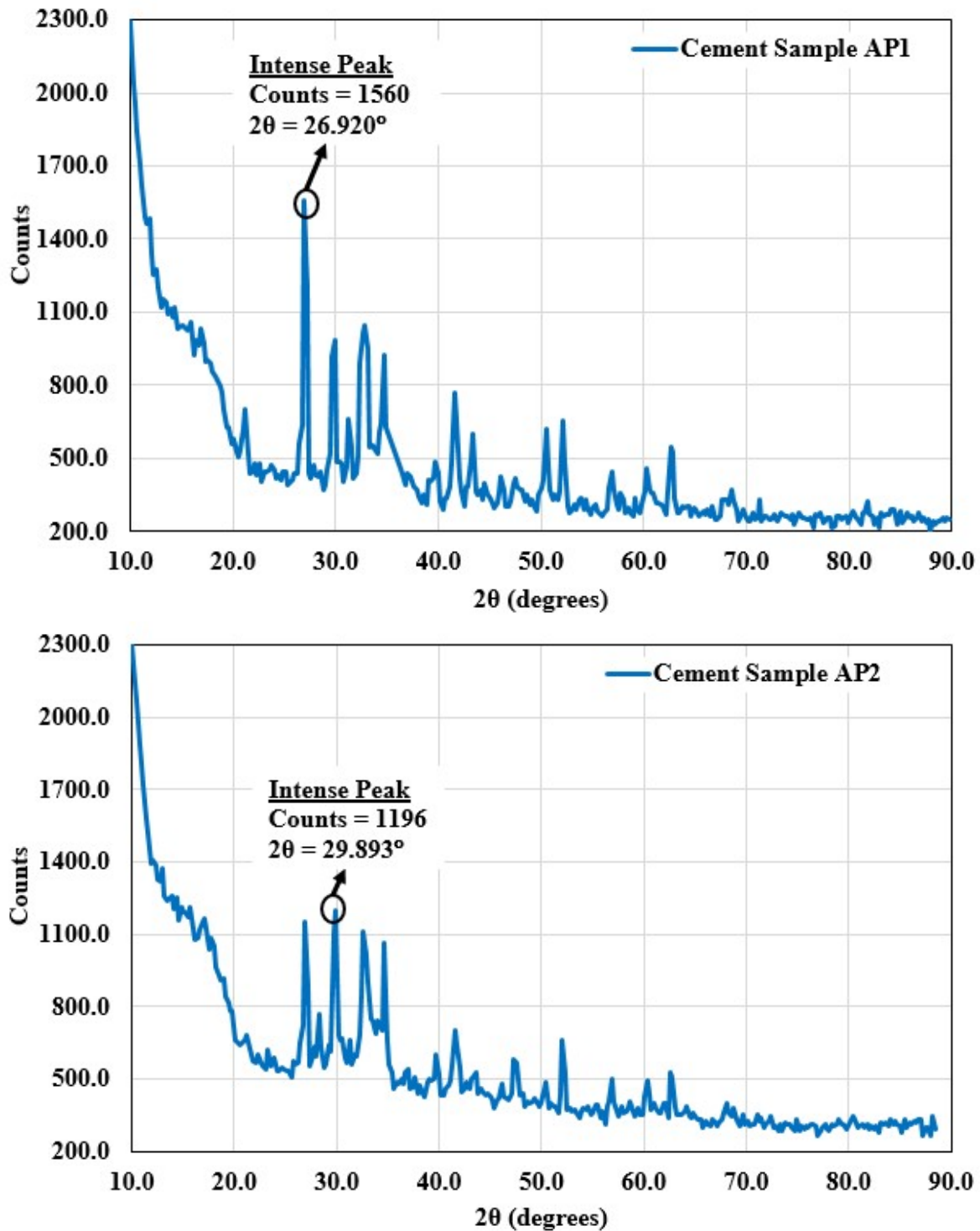


Figure 2. The XRD diffractograms for the cement samples (a) AP1, and (b) AP2. The most intense peaks assigned to the predominant crystallite phases are marked with their maximum count values and 2θ (degrees). The *Gaussian* convolution fittings for each of them are shown in Figure 4.

phases. The same angular range is corresponded to fly ash (CaO) phases as well. This diffraction band is

completely absent for the sample AP2, further suggesting its comparatively least amount alite phases in the granular cores. Few more sharp peaks appeared after the $2\theta_{max}$ of all the four samples such as at (a) $2\theta \approx 35^\circ$, a distinctive angle diffracted by the portlandite, alite, and belite ($2\text{CaO} \cdot \text{SiO}_2$ or Ca_2SiO_4) phases collectively; (b) $2\theta \approx 40^\circ$, an angle specific to the calcite phases; (c) $2\theta \approx 41\text{--}46^\circ$, a fingerprint angular region diffracted by the distinctive phases of the calcium silicates (alites and belites) and arsenates (primary $\text{CaH}_4(\text{AsO}_4)_2$, secondary $\text{CaH}(\text{AsO}_4)$, tertiary (normal) $\text{Ca}_3(\text{AsO}_4)_2$, and basic $\text{Ca}_5(\text{AsO}_4)_3\text{OH}$), aragonite ($2\theta \approx 46^\circ$) plus the gypsum $2\theta \approx 42^\circ$). At $2\theta \approx 41^\circ$, the specimen AP1 shows relatively more count (intense) peak than the others; confirming more amount calcium arsenate/silicate phases in its granular cores which means the AP1 brand would be more basic and aggressive subsequently to the iron bars and annealed iron wires reinforced into its concrete composites than others due to the alkaline chemical attack to the arsenate by $\text{Ca}(\text{OH})_2$ released successively from hydration chemical reactions [25] of it with water; (d) $2\theta \approx 50\text{--}52^\circ$, an angular regime diffracted collectively by the both portlandite and alite phases. In this region, the sample AP1 has the most prominent peaks followed by the AP4; a strong evidence decisive for claiming their portlandite and alite phases in relatively larger amount than that in the AP2 and AP3; (e) $2\theta \approx 55^\circ$, a distinguished angle diffracted only by the portlandite phases. In this angle, the sample AP3 has a negligible band, but the remaining three have considerable; deducing that AP3 shows the lowest extent of delivering that type of pozzolanic reaction products which are specifically initiated by the active involvement of the $\text{Ca}(\text{OH})_2$ unit of the portlandite phases [26], and offers the least contributions in modifying the carbonization resistance of the fly ash particulates [27] present originally into its granular cores, increasing the performance of the fly ash in terms of pore solution alkalinity of the cement-water pastes [28], preventing the weathering frequencies of

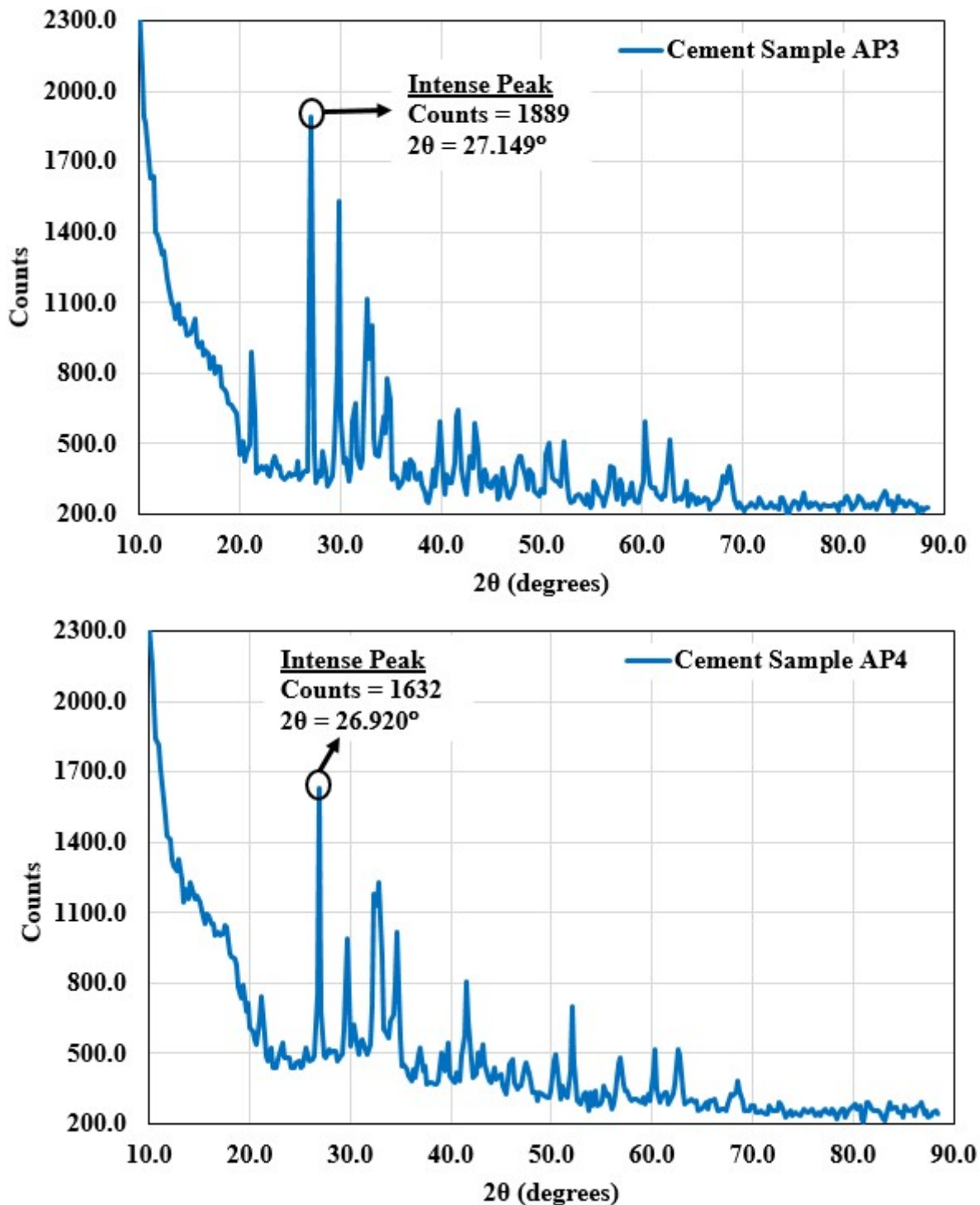


Figure 3. The XRD diffractograms for the cement samples (a) AP3, and (b) AP4. The most intense peaks assigned to the predominant crystallite phases marked with their maximum count values and 2θ (degrees). The *Gaussian* convolution fittings for each of them are shown in Figure 5.

the concretes due to salt attacks [29], enhancing the compressive strength [27, 29], controlling the stability of

the C–S–H (I) and C–S–H (II) gel matrices (hydration products), etc.; (f) $2\theta \approx 60\text{--}63^\circ$; a diffraction angular range distinctive for the hatrurite (Ca_3SiO_5) mineral sourced monoclinic alite phases (highly diffusive to the dopants such as P, Al, Si, Fe, Al, etc. uniformly). In this region, the specimen AP3 has the highest count peaks followed by AP1, but the rest two have almost negligible; elucidating that AP3 and AP1 are manufactured with the larger amount of non-clinker materials (fly ash, slag, and limestone are hatrurite enriched non-clinker materials) having contrastingly different thermochemistry, and recognizably better grinding energy savings, and lime saturation factor ($\text{LSF} = (\text{CaO} - 1.7 \text{ SO}_3) / (2.80 \text{ SiO}_2 + 1.18 \text{ Al}_2\text{O}_3 + 0.65 \text{ Fe}_2\text{O}_3)$). This type alite phase prevailed in the granular cores further unlock the possibility of modifying potential physicochemical properties of the AP3 and AP1 brands with substantial improvisations on their cementitious features by utilizing the potential *n*- and *p*- type dopants [30]. Beside this, the AP3 and AP1's monoclinic alite phases may offer relatively better hydration propensities with higher hydration index (HI (% by mass/hr.)), quick hardening potentialities with better strength index (SI) (*MPa/hr.*) [16], stronger binding effects to the aggregates and composite materials even at moderate temperature regimes [5], lower water penetration, permeability, absorption, and leakage [24], good sustainability to the concrete structures with significant decrement in hair cracking [31], considerable passivation effects on the reinforced iron bars/rods/sheets/wires, etc.; (g) $2\theta \approx 68\text{--}69^\circ$; a diffraction angle assigned specifically to the silica (α -quartz) SiO_2 phases. In this angle, the sample AP3 shows more count peaks followed by AP4, but the rest two have relatively negligible, suggesting that AP3 and AP4 brands have some extent of SiO_2 phases in their granular cores. In fact, in the early production stages of the PPC cements, some percentage by mass of the SiO_2 phases are impregnated into the clinker materials while standardizing the LSF scale, and are made very negligible or $< 1\%$ lately [31]. In terms of the mechanical strength and thermal expansion effects on the stabilized concrete made structures, the silica containing PPC cements are not preferably taken as good quality as it vigorously reacts with alkali ($\text{Ca}(\text{OH})_2$) produced during hydration chemical reactions of the cement with water, and forms the disruptive gel matrix having mechanical strengths worsening abilities. Accordingly, the crystallite silica content in the cement dusts creates high risk factor (occupational exposures) for chronic lung diseases and respiratory problems such as silicosis, lung cancer, air track inflammation, etc. Towards such rigorous factors, the AP3 and AP4 cement brands present themselves as relatively low quality brands than the AP2 and AP1; (h) $2\theta \approx 70\text{--}90^\circ$; none of the cement samples shows any of the spectral bands (Figure 6), confirming the complete absence of the Fe–C bonding traces ($2\theta = 75^\circ$ and 85°) (generated most probably during heating and quenching stages [32] of the kiln), alumina Al_2O_3 ($2\theta > 71^\circ$) [33], and ferrite Fe_2O_4 ($2\theta > 72^\circ$) [34] phases. Actually, the alumina and ferrite are preferably included in the manufacturing stages of the PPC cements in the course of stabilizing the clinker phases, and enhancing the calcination reaction efficiencies of the kilns at relatively low and high temperature regimes respectively, and are made null at the completion stages of the entire chemical reactions [31]. The complete absence of them in all the ready-to-use cement samples exemplifies their full consumptions in reducing kiln temperatures and CO_2 emissions steps of the manufacturing procedures.

Despite presenting series of the logical interpretations for and against to the quality assurance standardizations of the AP1, AP2, AP3, and AP4 PPC cement products, all these four brands are found to contain optimum level of calcium silicate (alite) as primary founding chemical phases along with belite,

calcite, portlandite, aragonite, vaterite, gypsum, and fly ash phases in significant amount plus the silica and calcium arsenate phases in the ultra-trace levels. And, their excessive yet precise inclusions in manufacturing Nepal made PPC cements make us to assure that all the four brands exhibit good cementitious features with

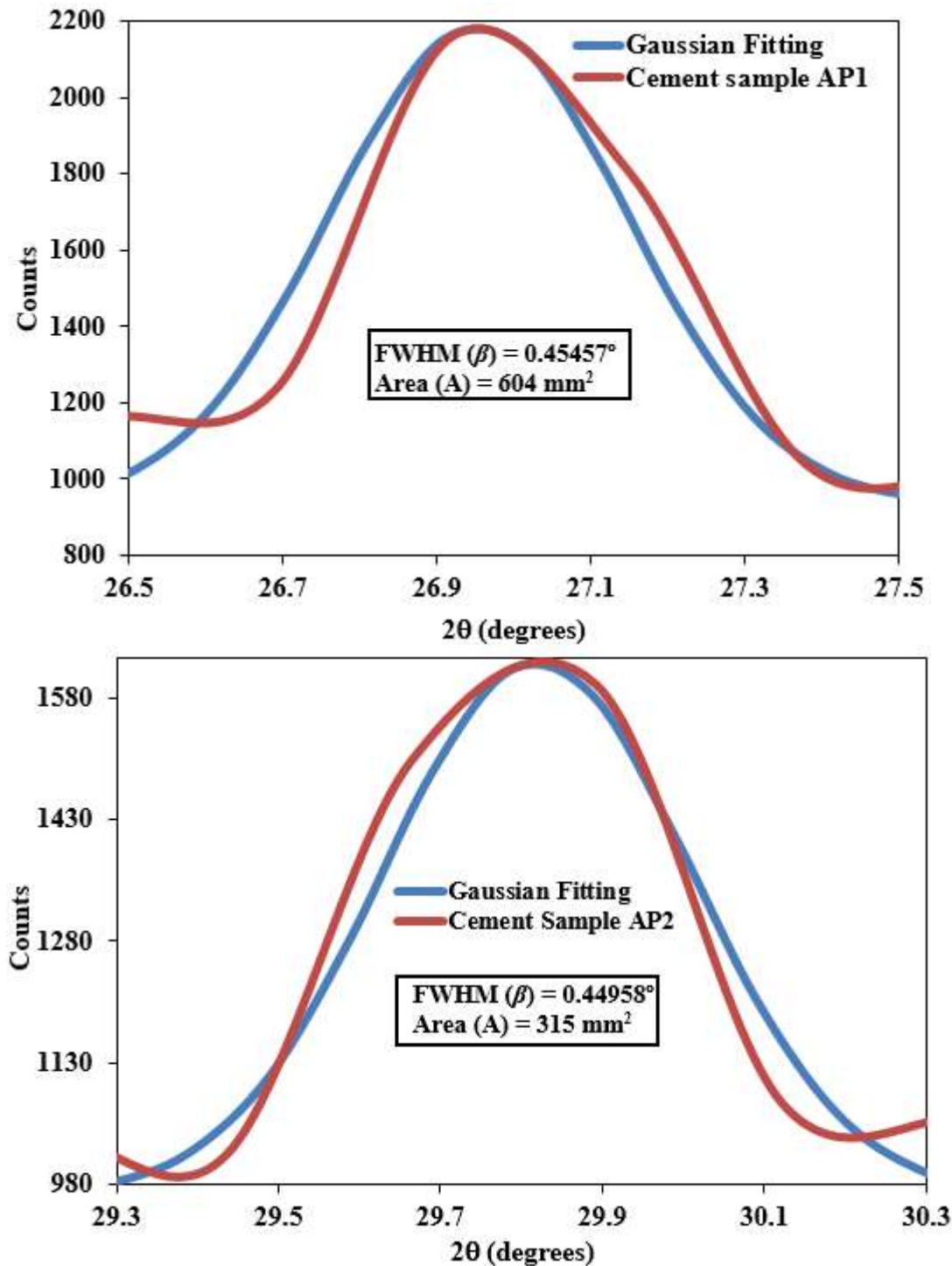


Figure 4. The *Gaussian* convolution fitting of the most intense XRD peak (marked in Figure 2) of the cement samples: (a) AP1 with $2\theta_{max} = 26.920^\circ$, and (b) AP2 with $2\theta_{max} = 29.893^\circ$. The concerned FWHM (β) and area (A) under the peaks determined through this peak fitting procedure are mentioned in the insets.

the effective incorporations of the natural and non-natural pozzolanic raw materials comprising with the wide

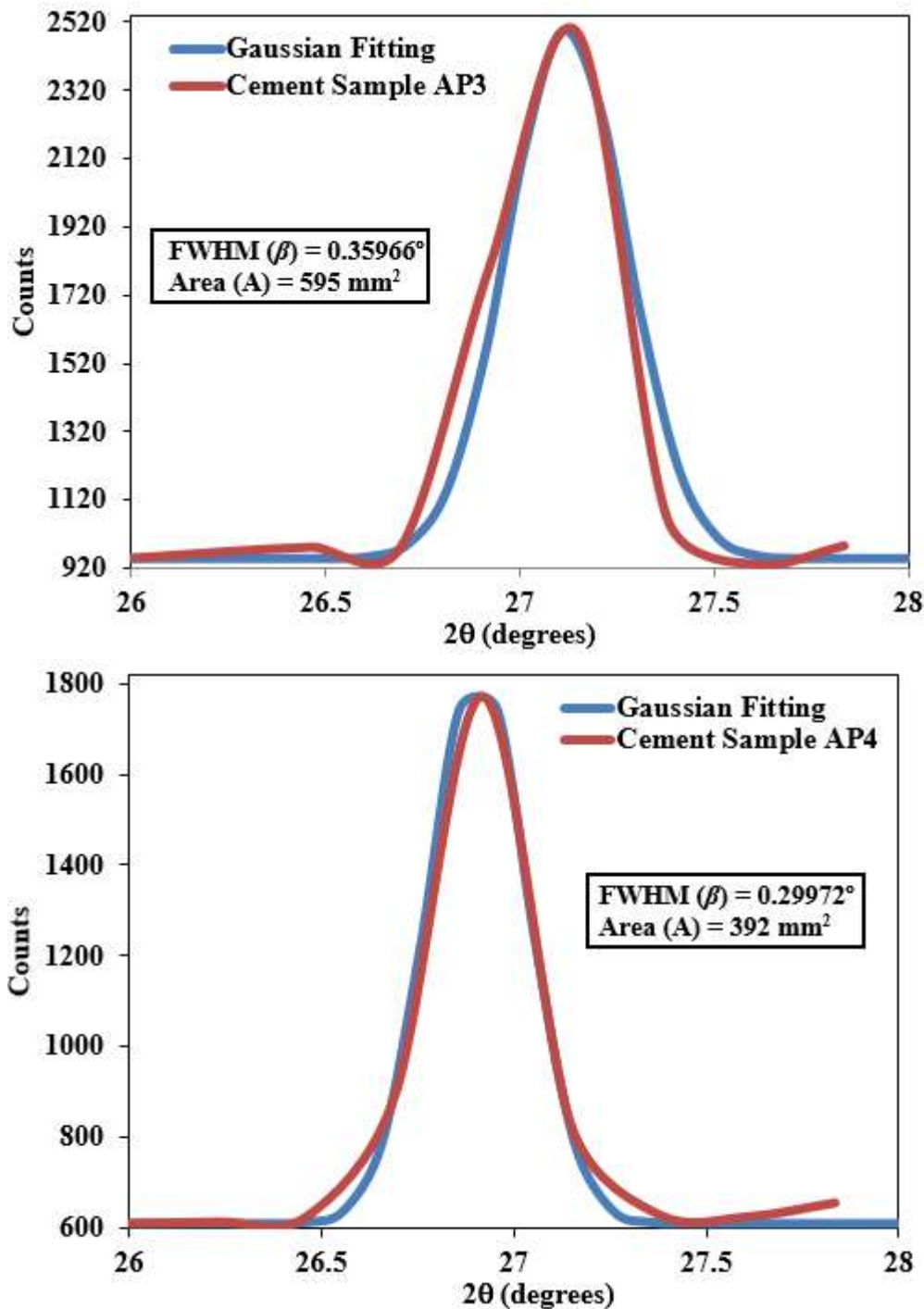


Figure 5. The *Gaussian* convolution fitting of the most intense XRD peak (marked in Figure 3) of the cement samples: **(a)** AP3 with $2\theta_{max} = 27.149^\circ$, and **(b)** AP4 with $2\theta_{max} = 26.920^\circ$. The concerned FWHM (β) and area (A) under the peaks determined through this peak fitting procedure are mentioned in the insets.

range crystallite phases. According to Bogue's composition of standardizing the cement-formulations for

acquiring better hydration reactions with good quality hydration products, the globally recommended doses for developing advanced PPC cement are alite (61%), belite (16%), aluminat ($\text{Ca}_3\text{Al}_2\text{O}_6$ or $3\text{CaO} \cdot \text{Al}_2\text{O}_3$ (C3A)) (10%), gypsum (CaSO_4) (6%), and ferrite ($4\text{CaO} \cdot \text{Al}_2\text{O}_3 \cdot \text{Fe}_2\text{O}_3$) C_4AF (8%) [31, 35]. In the context of these descriptive yet quality assurance ingredient ratios by mass as well, we claim that the Nepal made PPC cements have maintained good standards in their products.

In the course of determining interlayer distance d of each of those premier crystallite phases present in the AP1, AP2, AP3, and AP4 cements samples, the explicit diffraction angles $\theta^0 = 2\theta/2$; and $\theta_{max}^0 = 2\theta_{max}^0/2$ designated to them are substituted in Bragg's formulation (Eq. 1). The selected d values computed for their most predominant XRD bands (highest counts) raised at the dissimilar magnitude of the θ_{max}^0 are summarized in Table 1, wherein the FWHM (β) values estimated through the *Gaussian* convolution fitting techniques are also listed out. Those d values determined to their most predominant crystallite phases are 1.79Å, 1.98Å, 1.81Å, and 1.79Å respectively. These are the characteristic d -spacings to reconfirm the presence of the alite (triclinic /monoclinic) and calcite phases in all the four PPC cement samples. And, the concerned d values determined to their relatively less prominent phases with the distinguished XRD angle θ ($2\theta = 33^\circ, 21^\circ, 35^\circ, 40^\circ, 41^\circ, 42^\circ, 50^\circ, 51^\circ, 55^\circ, 60^\circ, 62^\circ$, and 69°) are 2.2Å (calcite), 1.4Å (alite), 2.2Å (gypsum), 2.3Å (portlandite, belite), 2.6Å (aragonite), 2.7Å (vaterite), 2.8Å (calcium arsenate), 3.2Å, 3.3Å (fly ash; CaO), 3.6Å, 3.8Å, 3.9Å, and 4.3Å (SiO_2) respectively; the quantitative descriptors just enough to reassure their portlandite, fly ash, belite, calcium arsenate/silicate, hatrurite (Ca_3SiO_5) derived alite (monoclinic), SiO_2 (α -quartz) type phases, but definitely of dissimilar quantitative proportions. If the literature values of the d determined for the wide range crystallite phases of the cements are referred in Å scale, all those d computed in this work are found as quite consistent. Few notable literature d spacings of the PPC cements relevant to the present study are (a) alite and calcite phases; $d = 1.60\text{--}3.04$ Å, (b) belite and calcite phases; $d = 2.1\text{--}2.7$ Å, (c) gypsum ($d = 2.3$ Å), (d) As^{5+} - bearing oxyanions (arsenate; AsO_4^{3-}); $d = 2.8\text{--}3.0$ Å, (e) portlandite phases; $d = 2.7$ Å, (f) aragonite and vaterite phases; $d = 2.7\text{--}2.9$ Å, (g) calcium arsenate phases; $d = 2.9$ Å, 2.2Å, and 2.9Å respectively, (h) ettringite phases (calcium aluminium sulfate) $\text{Ca}_6\text{Al}_2(\text{SO}_4)_3(\text{OH})_{12} \cdot 26\text{H}_2\text{O}$ (1 month old hydrated PPC cement); $d = 9.701, 5.630, 4.692, 3.875, 3.485, 2.773, 2.559, 2.219$ Å, (g) SiO_2 (α -quartz) phases; $d = 4.26$ Å [36–39]. If the packing tendency or ratio of the basal planes (deterministic to void volume) approximated for the predominant alite phases (representative d spacings derived from the $2\theta_{max}$ are 1.79Å, 1.98Å, 1.81Å, and 1.79Å) are considered, the four cement samples may follow the order: $\text{AP1} \approx \text{AP4} < \text{AP3} < \text{AP2}$.

Table 1. The Bragg's law and Scherrer's formula derived interatomic layer distance d , and crystallite size L of four different PPC cement samples AP1, AP2, AP3, and AP4.

Cement samples	XRD peak positions		Interlayer distance (d) (nm)	FWHM (β) ($^{\circ}$)	Area under the band (A) (mm^2)	Crystallite size L (nm)	No. of parallel planes (m)
	$2\theta_{max}^{\circ}$	θ_{max}°					
AP1	26.920	13.460	0.179	0.45457	604	18.76	104.6
AP2	29.892	14.946	0.199	0.44958	315	19.09	96.1
AP3	27.149	13.574	0.181	0.35966	595	23.72	131.2
AP4	26.920	13.460	0.179	0.29972	392	28.45	158.6

In terms of the size of the predominant crystallite phases L and the overall granular morphological analyses plus the agglomerating propensities of the crystallites and grains, the precise rankings of the presently selected four cement specimens always forecasts more rigorous explanations descriptive to their realistic physical observables such as packing tendencies and void volume, weight and density, water absorption and hydration reaction trends, and the overall placing, adhering, setting, and enduring potentialities, etc. The same size dependencies of the granular level crystallites are responsible to depict the periodical frequency of post-curing/ treatment of the PPC cement made structures with water. The Scherrer's formula (Eq. 2) is the only mathematical mean that can approximate L and the overall average range of particle distributions quantitatively. While the specific values of the constant K (Eq. 3), and the variables such as FWHM (β) (Figure 4 and Figure 5), diffraction angle ($2\theta_{max}/2$) of the predominant crystallite phases (alite) of the AP1, AP2, AP3 and AP4 cement samples are substituted explicitly in Eq. 2, the crystallite sizes L are computed as 18.76 nm, 19.09 nm, 23.72 nm, and 28.45 nm respectively (Table 1). These values are significantly smaller than those determined for the OPC cements of the same manufacturers (AP3 (OPC) = 34.58 nm; and AP4 (OPC) = 32.44 nm) as reported by the present author elsewhere [13]; which is however very obvious and convincible as the in-built granular phases of the PPC cements are composed with the contrastingly different yet enormous amount ash and pozzolanic type materials holding extra fine particulates, and are produced with the excellent control over burning and grinding conditions that only allow to hold maximum extent of alite and porlandatite phases. Based on the same L , the four cement specimens follow the order: AP1<AP2<AP3<AP4; suggesting that the sample AP1 contains more extra fine grain particulates with the lowest average particle size distributions range. If the size dependent growth and agglomeration mechanisms of the crystallites into the grain cum particles are referred, the smaller crystallites always lead to the development of relatively smaller grain cum particle sizes. Therefore, the average size distributions of the grain cum particles dispersed into the grainy matrices of the four specific cement brands would be in the order AP1<AP2<AP3<AP4 provided that the intensive effects of the humidity, temperatures, packing coefficients,

and granular compositions are avoided practically. If the number of the parallel interatomic planes (m) of the predominant alite phases that remain completely stacked one over the other; an indicator decisive for verifying the actual thickness of the crystallites practically, determined herewith (Eq. 4) for the AP1, AP2, AP3, and AP4 cement samples (approximately as 105, 96, 131, and 159 respectively (Table 1)) are referred, the order would be $AP2 < AP1 < AP3 < AP4$. Similarly, in terms of these L values owing to exhibit good intermixing propensities with the nano sized carbon powders ($L = 2\text{-}12\text{ nm}$), all these four PPC cements could be taken as the best prototype candidates for inventing low cost capacitors and conductive devices. Additionally, towards the recent worldwide practices of enhancing compressive strength of the cements by impregnating 5 to 40 % of the carbon dust by weight of the cement [39, 40], all these four PPC cements may serve as potential binders to the latter. In fact, the underlying principle that explains both of these applicative features practically is: the intermixing tendencies of the two or more than two dissimilar material particles (in this case, cement and carbon) into their own interstitial sites or the trends of the materials diffusions are solely depend on their explicit granular sizes, and the more homogeneous diffusions are likely to occur if the particulate sizes of the intermixing materials resemble well. Besides these, the presently computed granular sizes and the thickness of the crystallite particulates also exemplify that the designated manufacturers/depos of the AP1 and AP2 cements have to adopt more particle suppression/dust-free technologies in their industrial plants with the effective implementations of more rigorous safety precaution guidelines than that for the AP3 and AP4. Nevertheless, either of the four manufacturers ($L < 30\text{ nm}$) are required to make the compulsion of using high quality face masks with extraordinary sealing technology, super protective face shields, eyes & skin protectors, etc. to their industrial workers in order to minimize the occupational health risks. Since, the entire industrial manufacturing strategies and the workers' safety guidelines implemented throughout the individual production plants are not publicly accessible, the critical criticisms based on the present interpretations would

be impracticable rather making them alert to maintain the effective measures and to remain vigilant towards the futuristic occupational hazards.

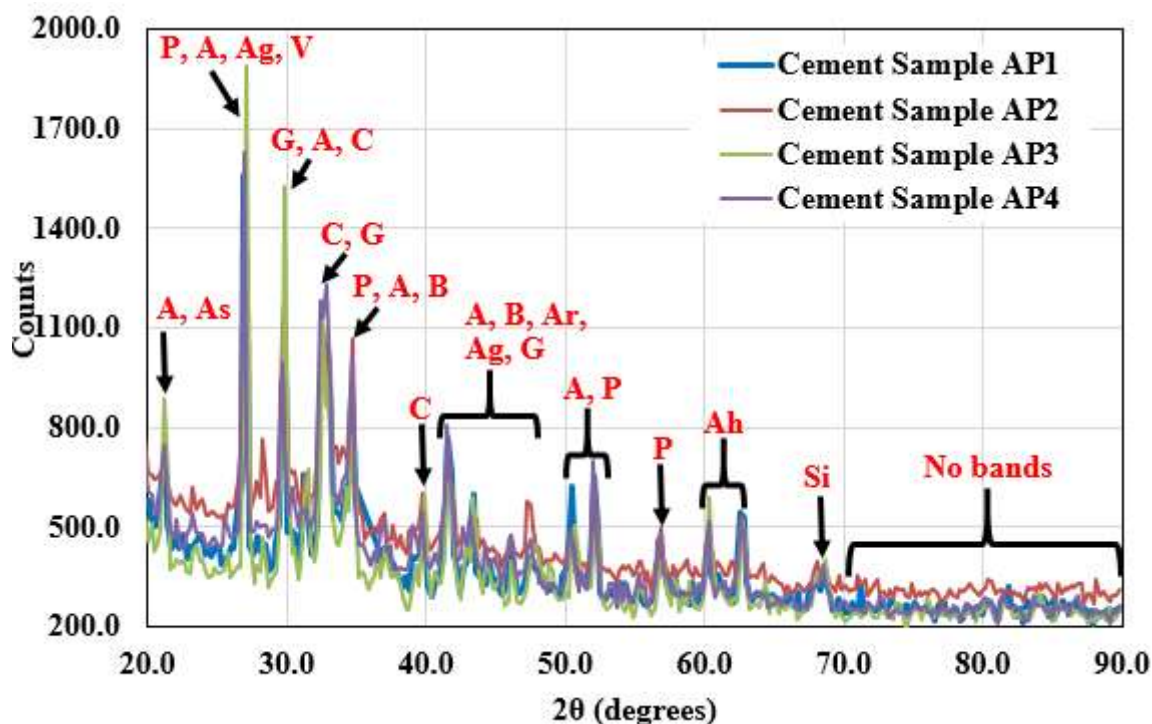


Figure 6. The XRD diffractograms for all the four cement samples AP1, AP2, AP3, and AP4. The specific bands of each sample at distinctive diffraction angles ($2\theta_{max}$ and 2θ) are characterized explicitly: (Abbreviations: A = Alite, B = Belite, C = Calcite, G = Gypsum, Ag = Aragonite, V = Vaterite, P = Portlandite, As = Fly ash, Ar = Arsenate, Ah = Alite (Hatrurite), Si (Silica (α -quartz))).

Alike to those crystallite size L dependent interpretations of the potential physicochemical properties, the rates at which the PPC cements and cement made materials absorb water into their interstitial sites, and the propensities of them to dispense various type succeeding hydration reaction products as a function of hydration reactions time with water are also directly influential parameters. Normally, more fine grains cum particles possess relatively higher specific surface areas because of which many layers of the hydration products get adsorbed successively and intensified the subsequent hydration kinetics. And, the extent to which granular packing ratio of the crystallite phases is maintained in the cement materials is vowed to determine compressive strength and evaporable water (absorbed and capillary) retaining potentialities. Therefore, the more fine is the grain cum particle size of the cement, the quicker would be the heat of hydration and hydration kinetics with the rapid acquiring of the distinguished hydration reaction products. Thus, the hydration reaction trends of the present four cement specimens can be speculated as $AP1 > AP2 > AP3 > AP4$ as the former two ($AP1: L = 18.8 \text{ nm}$, $AP2: L = 19.1 \text{ nm}$) exhibits a speedy hydration reaction rates than that of the latter ($AP3: L = 23.7 \text{ nm}$, $AP4: L = 28.5 \text{ nm}$). This rate, however is subjected to change if the in-depth instrumental

characterizations of the hydration reaction products of the every cements released from the very early (fresh paste) to late hydration stages (hardening) are carried out. Just like this, some other cementitious (placing, setting, adhering, enduring) propensities of the cement-water-sand-pebble pastes in fresh, moderate, and late stages are also reliable to the size of their founding crystallite grains and their distribution ranges. In principle, if the cements hold predominant number densities of the finest grains cum particles (but, not in ultrafine levels), the setting rates of them become more prompts. It is highly beneficial to underscore herewith that the cements with good range particle size distributions are globally demanded in order to meet the needs of various state-of-art engineering designs/ architectures. Practically, the average size range by which the entire particles of the cements get distributed is directly measurable (particle size analyzer) observable, however, the presently determined variable L of the predominant crystallite phases of the AP1, AP2, AP3, and AP4 cements depict the approximate size range of their agglomerated grains cum particles as $AP1 < AP2 < AP3 < AP4$, and hence the cementitious features offered by them would follow the order $AP1 > AP2 > AP3 > AP4$.

Despite underscoring all those crystallite size dependent measurable observables required to inspect the quality assurance norms of the commercially available variable technology made Nepalese PPC cements plus their immediate consequences associated with the dissimilar crystallite sizes (L) and thickness (m), grain cum particle sizes/distribution ranges, packing coefficients and basal spacings (d), hydration propensities and cementitious abilities, etc., all the four PPC brands (AP1, AP2, AP3, AP4) selected herewith preferentially are expected to dispense significant workability and compressive strength, satisfactory setting and enduring muscularity, reasonably low risks of hair cracking and high passivation effects over the reinforced iron bars, quick hydration kinetics with good quality hydration reactions products, etc. And, all these publicly desirable yet quality assurance indicators associated with the commercially available Nepal made PPC cements assed through the XRD characterizations techniques verify that none of the four cement brands have at least violated the standard manufacturing norms and basic formulations of the clinker phases required to be enriched with portlandite, alite, belite, arsenates/silicates, polymorphs of calcite, fly ash, gypsum, etc. The supplementary yet additional evidences indispensable to prove all those predominant, premier, subsidiary, and ultra-traces chemical phases lying in the granular cores of four PPC cement brands are presented in subsection 3.3.

3.3 Interpretations of the FTIR Spectrograms

The Fourier Transform Infrared (FTIR) spectroscopy is as multidimensional attributes offering instrumental characterizations technique as XRD whose fundamental principle is, however, aligned firmly in tracing out those type chemical bonds of the molecular fragments that undergo vibrational transitions with significant changes in dipole moments (IR active). Since the dipole moment is a typical characteristic feature of the heteroatomic chemical bonds, and the chemical moieties made up of two or more than two contrastingly different electronegative atoms bonded each other with two oppositely charged electric poles, the prompt instrumental detections and recordings (IR spectrum) of the specific IR frequency absorption regions of their selected IR active vibration modes are deterministic to the precise identifications of their chemical bonds and moieties. Alike to the wide range engineering materials and many other polymeric motifs, all type cements and cement made products contain various type of the chemical phases and distinguishable chemical moieties holding wide range heteroatomic functional groups, charged and uncharged radicals, neutral molecules, etc.

as they are manufactured with relatively low cost natural and non-natural raw materials (clinkers) industrially, and are derived as finely refined ultra-dust phases possessing remarkable cementitious features [13]. More particularly, the PPC brand cements are manufactured with the unique formulations of the clinker phases inclusive with the pozzolanic materials, slags, natural and organic fly ashes, gypsums, silicates/arsenates of calcium, polymorphs of calcites, etc., for the preferential usage of them to those specific engineering designs /architectures where the normal OPC cements cannot fulfill the required functional demands. Therefore, it's doubtless to consider their heteroatomic chemical moieties and chemical phases practically as IR detectable. However, the proper characterizations of them in the variable technology produced PPC cements always guaranties the associated measures indispensable for assuring their qualities and potential physicochemical properties. Similar to the XRD spectroscopy technique (subsection 3.2), the FTIR measurement equally offers granular-characterizations skills which in fact discloses additional verifications required to probe the chemical bonds and bonding fragments/segments appended to the crystallite phases predicted by the former. Thus, the following FTIR spectroscopy characterizations of the Nepal made variable brands AP1, AP2, AP3, and AP4 PPC cements bring the quality assurance of the latter into repute to the commercial markets.

The FTIR spectra measured for the AP1, AP2, AP3, and AP4 are displayed in Figure 7 where the intense IR bands having maximum percentage transmittance (% T) raised at $\sim 420\text{ cm}^{-1}$, $\sim 800\text{ cm}^{-1}$ – $\sim 1100\text{ cm}^{-1}$, $\sim 1435\text{ cm}^{-1}$, $\sim 2360\text{ cm}^{-1}$, and $\sim 3650\text{ cm}^{-1}$ absorption frequency regimes are encircled by the oval shapes. All these sharp IR active bands plus the few more additional diffusive bands are identified herewith explicitly by referring the standard databases mentioned in the scientific literatures [13, 15, 16, 36–41], and the associated digital-libraries designated to the IR spectral analyses. The very first IR active band of all the four cement specimens appeared at $\sim 420\text{ cm}^{-1}$ is very much specific to the IR active Ca–O bond vibration modes. This observation is a strong evidence of claiming CaO (fly ash) as one of the potential crystallite phases of all of them as predicted by the XRD spectroscopy. In terms of the approximate quantitative amount of this phase speculated from the depth intensity of the concerned IR bands, the four cement samples can be arranged as: AP2>AP3>AP1>AP4. The subsequently intense yet mostly broadened three active bands raised at $\sim 520\text{ cm}^{-1}$, $\sim 670\text{ cm}^{-1}$, $\sim 713\text{ cm}^{-1}$, and $\sim 875\text{ cm}^{-1}$ wave number regions correspond to the symmetric bending vibration modes of the Si–O–Si (shifted from $\sim 450\text{ cm}^{-1}$ region due to gypsum as an ingredient), stretching S–O vibrations of SO_4^{2-} unit of gypsum (MgSO_4 –fly ash/slag matrix), CO_3^{2-} deformation vibrations in aragonite, and out of plane bending mode of the CO_3^{2-} part ($\nu_2\text{ CO}_3^{2-}$) in light calcite (CaCO_3) and its closely associated crystallite phases respectively. Additionally, few more moderate to weak yet broadened bands appeared at (a) $\sim 880\text{ cm}^{-1}$ justifies the presence of As^{5+} –bearing oxyanions ($\nu_3\text{ AsO}_4^{3-}$) holding calcium arsenate compounds (primary ($\text{CaH}_4(\text{AsO}_4)_2$), secondary ($\text{CaH}(\text{AsO}_4)$), tertiary (normal) ($\text{Ca}_3(\text{AsO}_4)_2$), and basic ($\text{Ca}_5(\text{AsO}_4)_3\text{OH}$)), and out-of-plane CO_3^{2-} bending vibrations in vaterite; (b) $\sim 920\text{ cm}^{-1}$, a region for the IR active asymmetric Si–O stretching vibration modes of the predominant alite (Ca_3SiO_5) and subsidiary belite (Ca_2SiO_3) phases; (c) $\sim 970\text{ cm}^{-1}$, specific to the asymmetric stretching of the Si–O bond of calcium silicate hydrate Ca (Si–O–H); (d) $\sim 1000\text{ cm}^{-1}$, $\sim 1100\text{ cm}^{-1}$, and $\sim 1120\text{ cm}^{-1}$ the characteristic absorptions $\nu_3\text{ SiO}_4^{4-}$ & $\nu_3\text{ SiO}_4^{2-}$ of the tetrahedral moieties of the silicates and their polymerized networks (orthosilica ($\text{Si}_2\text{O}_7^{6-}$), CO_3^{2-} stretching vibrations in aragonite, and SO_4^{2-} radicals in

the gypsum. The next sharpest spectral band of all the four cement samples appeared at $\sim 1435 \text{ cm}^{-1}$ ($\nu_2 \text{ CO}_3^{2-}$) is due to the stretching C–O vibration modes of the CO_3^{2-} unit, indicative to the assurance of CO_3^{2-} and CO_3^{2-} holding chemical moieties (polymorphs of CaCO_3 : calcite, aragonite, and vaterite) as one of the most significant crystallite phases. Similarly, the quite diffused peaks appeared at $\sim 470 \text{ cm}^{-1}$ and $\sim 1100 \text{ cm}^{-1}$ are due to the bending vibration modes of the Si–O–Si and asymmetric stretching modes of the Si–O respectively, which in turn act as a standalone evidence of declaring SiO_2 (α -quartz) as an ultra-trace silica phase (alike to XRD observations). If the net peak-depth area are approximated explicitly, the different sample specimens contain different quantitative amounts of the SiO_2 phases, but certainly of trace levels. Moreover, the relatively less % T & diffused, and the most % T & intense peaks at $\sim 1795 \text{ cm}^{-1}$ and $\sim 2370 \text{ cm}^{-1}$ further illuminated the calcite as one of the subsidiary crystallite phases: the former band corresponds to C=O vibration modes of the CO_3^{2-} segment while the latter corresponds to the stretching modes of its O–C–O and CO_2 (atmospheric infusion of the CO_2 to the just collected cement powders (or in perfectly unsealed/unpacked conditions) add some traces of CaCO_3 as; $\text{Ca(OH)}_2 + \text{CO}_2 \rightarrow \text{CaCO}_3 + \text{H}_2\text{O}$). Again, the next less %T bands of each sample

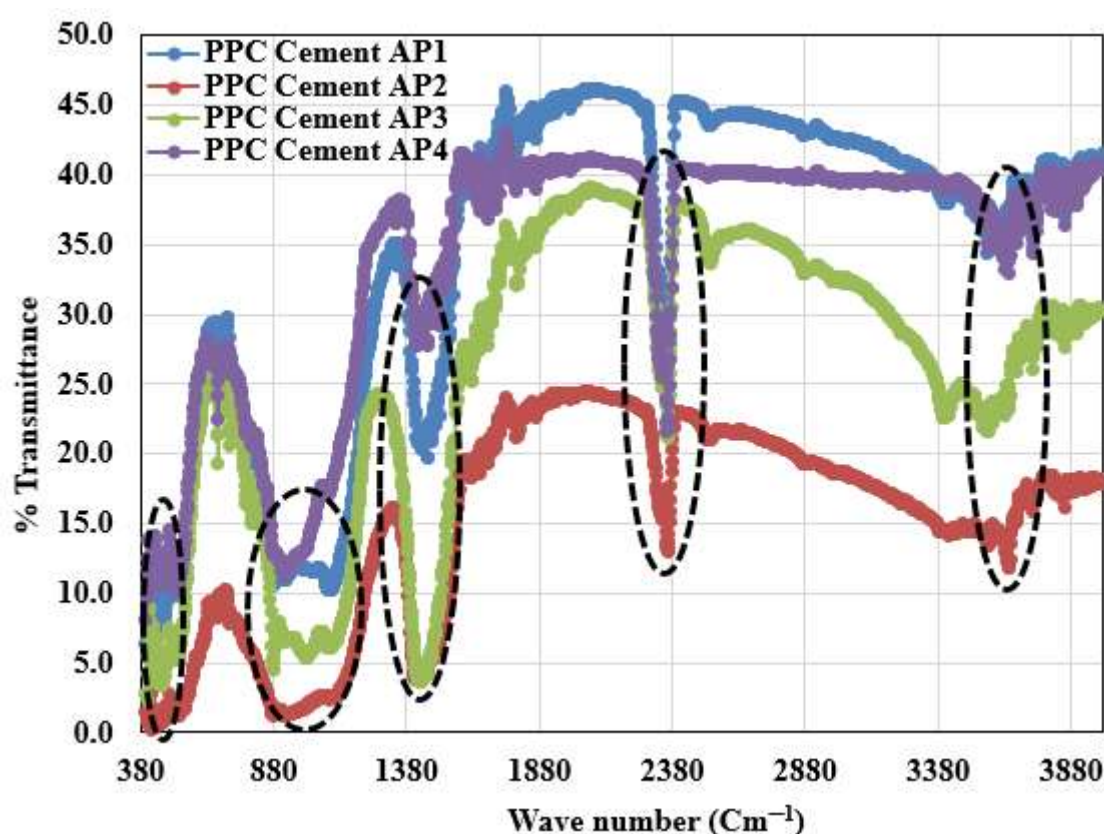


Figure 7. The IR spectra of the cement samples AP1, AP2, AP3, and AP4 measured with the Shimadzu IR Affinity-1S (S.No.AZ1965904022) spectrometer. The most intense IR peaks of all the samples appeared at wave numbers $\sim 420 \text{ cm}^{-1}$, $\sim 800 - \sim 1100 \text{ cm}^{-1}$, $\sim 1435 \text{ cm}^{-1}$, $\sim 2360 \text{ cm}^{-1}$, and $\sim 3650 \text{ cm}^{-1}$ are encircled by the oval shapes.

appeared at $\sim 2520\text{ cm}^{-1}$ and $\sim 2880\text{ cm}^{-1}$ are due to the combinational vibration modes, viz.; (v_3+v_4) and $2v_3$ of the CO_3^{2-} unit in CaCO_3 polymorphs, but the similar type band at $\sim 3412\text{ cm}^{-1}$ is due to the asymmetric stretching vibrations of the O–H and H–O–H of the water molecules released either from the high pressure phases of the hydrous mineral, viz.; portlandite $\text{Ca}(\text{OH})_2$ phases (they have layered structures with the layered OH^-) or of the crystal waters of the hydrated calcites ($\text{CaCO}_3 \cdot n\text{H}_2\text{O}$) and gypsums ($\text{CaSO}_4 \cdot 2\text{H}_2\text{O}$) or the hydrogen bond bound OH groups (H---O–H). Furthermore, the last, second last, and the third last IR bands (relatively very weak and less intense) of all the four sample specimens appeared at $\sim 3850\text{ cm}^{-1}$, $\sim 3645\text{ cm}^{-1}$, and $\sim 3430\text{ cm}^{-1}$ respectively corresponds to the C–H bonds vibrations of their organic traces sourced from the impure natural and non-natural pozzolanic raw materials, O–H stretching vibration modes of the portlandite ($\text{Ca}(\text{OH})_2$), and ($v_1 + v_3$: H_2O) combinational vibration modes of the H_2O (to some extent, the molecular level water is likely to be adsorbed/absorbed on the surface of the cement particulates in the sampling step itself) and H-bound OH (H–OH) segments. More especially, the second last absorption frequency range is very typical to the low degree carbonated cement samples, but enriched with the portlandite phases.

Alike to the above confirmations of all the XRD spectroscopy revealed crystallite chemical phases and their covalently bonded chemical moieties holding different types active heteroatomic functional groups/segments, the absolute absence of some unwanted phases, but typical to other types cements (magnetite, boehmite, pseudoboehmite, magnesia, $[(\text{Al})\text{O}_4]^{5-}$ & $[(\text{Fe})\text{O}_4]^{5-}$ moieties, calcium tetrahedra-aluminoferrite, AlO_4 tetrahedra, Si–OH segments, etc.) can also be assed quantitatively. Actually, the general PPC type cements should not hold such type crystallite phases practically, and must not utilize these phases enriched clinkers as their raw materials, and if they were incorporated intentionally/accidentally even as trace levels, the workability of the PPC cements is worsen considerably. Therefore, the close inspections of them unveils few valuable assets needful for assuring entire qualities of the PPC cements. As shown in Figure 6, none of the AP1, AP2, AP3, and AP4 specimens produce the typical IR bands raised at (a) $\sim 550\text{ cm}^{-1}$ (Fe–O vibration), and $\sim 1070\text{ cm}^{-1}$ (Al–O–H vibrations): describing the null presence of magnetite (Fe_3O_4) and boehmite ($\text{AlO}(\text{OH})$) minerals and their chemical traces; (b) $\sim 554\text{ cm}^{-1}$ (Al–O–OH bending vibration), and $\sim 465\text{ cm}^{-1}$ (Al–O stretching): ensuring the complete absence of the pseudoboehmite ($\text{AlOOH} \cdot n\text{H}_2\text{O}$) type aluminium mineral and the associated chemical traces; (c) $\sim 548\text{ cm}^{-1}$ (Mg–O stretching): confirming no holdings of the magnesia (MgO) and MgO based chemical compounds (magnesia powder is sometimes used as additives to reduce the atmospheric CO_2 diffusivity into the cement powders); (d) $\sim 600\text{ cm}^{-1} - \sim 800\text{ cm}^{-1}$, and $\sim 800\text{ cm}^{-1} - \sim 830\text{ cm}^{-1}$: declaring no indications of the Al–O and Fe–O stretching vibration modes of $[(\text{Al})\text{O}_4]^{5-}$ & $[(\text{Fe})\text{O}_4]^{5-}$ chemical moieties, and calcium tetrahedra-aluminoferrite ($4\text{CaO} \cdot \text{Al}_2\text{O}_3 \cdot \text{Fe}_2\text{O}_3$; C_4AF) phases respectively; (e) $\sim 820\text{ cm}^{-1}$, and $\sim 705\text{ cm}^{-1} - \sim 780\text{ cm}^{-1}$: signifying no traces of the AlO_4 tetrahedra, and $\sim 845\text{ cm}^{-1}$: reconfirming no Mg–O derived magnesia additives; (f) $\sim 1610\text{ cm}^{-1} - \sim 1630\text{ cm}^{-1}$: indicating nil concentrations of the Si–OH chemical moieties. All these null amount detections of the low quality minerals, chemical phases, and the heteroatomic chemical moieties plus functional groups ensured us that no granular worsening effects of them on the in-built ultra-fine grainy matrices (gypsum/fly ash/slag/pozzolanic) of the AP1, AP2, AP3, and AP4 PPC cement brands exists, and hence, all are

recommended as reputable brands following the specific standard norms of their basic formulations and the founding chemical compositions of the clinker phases & the associated raw materials adopted in NS code.

4. CONCLUSION

Nepal, being a developing country with various ongoing mega construction projects nationwide, hosts foreign installed, state-owned, and the privately financed cement industry produced dissimilar brand OPC, PPC, and PSC cements regulated under the integral policy of Nepal Standard (NS) code. Among these cements branded across the nation, the PPC brands rank first with 50% occupancy of the gross cumulative productions, and cover major stakeholders of the national pride engineering constructions, exporting/importing trends to/from the neighboring countries, Nepalese dynamic commercial markets, and the total budget injected into the cement industries. On the one hand, the NS code and its standard manufacturing guidelines are strictly implemented throughout the PPC production plants, the modern formulations of the pozzolanic raw materials and the clinker phases are firmly standardized, the smooth supply of the needful ingredients from the foreign lands is very much regularized, and the suitability of the industrially adopted production technologies is periodically inspected, but on the other hand, Nepalese people around the nation are frequently complaining about the quality of the PPC products prevailing mostly in their commercial markets, and sometimes are reluctant to use them confidently with the good hope of acquiring better workability, high compressive strength, recognizable enduring ability, low corrosive attacks on the reinforced iron/steel bars and annealed iron wires even under the aggressive environmental conditions, remarkable compactness with low risks of hair-cracking, better resilience towards thermal expansion/contraction effects, less frequent post-treatment/curing attentions, etc. Besides these, even the existing PPC cement production plants both in the operated/non-operated conditions throughout the nation are constantly looking for the continuous pace of the development, advancement, improvement, and innovations of the modern type PPC cements with standard quality pozzolanic phases in order to meet their products to international standards and public desires. The only means that can minimize these industry-academia gaps practically, and address the underlying challenges significantly with the genuine productions of the quality products of PPC is to intensify R & D investigations in revealing their fundamental founding crystallite phases followed by the required improvisations on their clinker formulations. In this contribution, we incorporated a number of measures required to assess the quality assurance of the four publicly desired variable technology made ready-to-use ultra-dry Nepalese PPC cement products (designated samples: AP1, AP2, AP3, and AP4) quantitatively, and investigated their founding clinker particulates/phases, exclusive roles of the predominant particulates and their porosities plus crystallite sizes, crystallite chemical phases and the degree of their compactness (packing ratio), chemical constituents and the types of the functional groups, etc. through X-ray diffraction (XRD) and Fourier Transform Infrared (FTIR) spectroscopy techniques.

We at first confirmed all the founding crystallite phases of the PPC cements required to be incorporated into their clinker formulations by the XRD technique followed by the critical evaluations on the interlayer spacing (d) (Å) computed to each explicit phase through the Bragg's formulation. The particular diffraction angles deterministic to all the premier crystallite phases of the dry ready-to-use AP1, AP2, AP3, and AP4

cement dusts were: (a) $2\theta_{max} = 26.920^\circ$, 29.893° , 27.149° , and 26.920° : fingerprint regions for portlandite ($\text{Ca}(\text{OH})_2$), alite ($3\text{CaO} \cdot \text{SiO}_2$ or Ca_3SiO_5), gypsum (CaSO_4), and aragonite & vaterite (polymorphs of CaCO_3); (b) $2\theta \approx 33^\circ$: specific to gypsum, and calcite (CaCO_3), (c) $2\theta \approx 21^\circ$: corresponds to fly ash (CaO) and alite type silicates; (d) $2\theta \approx 35^\circ$: particular to portlandite, alite, and belite ($2\text{CaO} \cdot \text{SiO}_2$ or Ca_2SiO_4) type silicates; (e) $2\theta \approx 41\text{--}46^\circ$: corresponds to gypsum, calcium silicates (alites & belites), calcium arsenates, and aragonite; (f) $2\theta \approx 50\text{--}52^\circ$: diffraction caused collectively by portlandite and alite; (g) $2\theta \approx 55^\circ$: specific to portlandite; (h) $2\theta \approx 60\text{--}63^\circ$: distinctive to hatrurite (Ca_3SiO_5) mineral derived alite (monoclinic); and (i) $2\theta \approx 68\text{--}69^\circ$: fingerprint regime to silica (α -quartz) (SiO_2). Thus speculated founding chemical phases were also firmly ensured with their calculated basal spacing (d) values: alite ($d = 1.4\text{--}1.8 \text{ \AA}$), calcite ($d = 2.2 \text{ \AA}$), portlandite & belite ($d = 2.3 \text{ \AA}$), gypsum ($d = 2.2 \text{ \AA}$), aragonite ($d = 2.6 \text{ \AA}$), vaterite ($d = 2.7 \text{ \AA}$), calcium arsenate ($d = 2.8 \text{ \AA}$), fly ash ($d = 3.3 \text{ \AA}$), and silica ($d = 4.3 \text{ \AA}$). Besides these, the most predominant chemical moieties and the heteroatomic chemical bonds bound functional groups/segments held into the granular cores of all those crystallite phases were also searched out by FTIR instrumental method. The most typical IR active band/s appeared at different absorption frequency (wave number) regimes stood as standalone evidences to theorize each of those chemical phases quantitatively, viz., (a) $\sim 420 \text{ cm}^{-1}$: Ca–O vibration modes (CaO (fly ash)); (b) $\sim 520 \text{ cm}^{-1}$, $\sim 670 \text{ cm}^{-1}$, $\sim 713 \text{ cm}^{-1}$, and $\sim 875 \text{ cm}^{-1}$: symmetric bending vibration modes of Si–O–Si (silica), stretching S–O vibrations of SO_4^{2-} (gypsum (CaSO_4)), CO_3^{2-} deformation vibrations (aragonite), and out of plane bending mode of CO_3^{2-} (light CaCO_3 /calcite phases); (c) $\sim 880 \text{ cm}^{-1}$: As–O vibration modes of AsO_4^{3-} (calcium arsenate) and out-of-plane CO_3^{2-} bending vibrations (vaterite); (d) $\sim 920 \text{ cm}^{-1}$: asymmetric Si–O stretching vibration modes (alite (Ca_3SiO_5) and belite (Ca_2SiO_4)); (e) $\sim 970 \text{ cm}^{-1}$: asymmetric Si–O stretching (calcium silicate hydrate $\text{Ca}(\text{Si–O–H})$); (f) $\sim 1000 \text{ cm}^{-1}$, $\sim 1100 \text{ cm}^{-1}$, and $\sim 1120 \text{ cm}^{-1}$: $\nu_3 \text{SiO}_4^{4-}$ & $\nu_3 \text{SiO}_4^{2-}$ modes (tetrahedral silicates and their polymerized orthosilica ($\text{Si}_2\text{O}_7^{6-}$)), CO_3^{2-} stretching vibrations (aragonite), and SO_4^{2-} asymmetric stretching (gypsum); (g) $\sim 1435 \text{ cm}^{-1}$: stretching C–O vibration modes ($\nu_2 \text{CO}_3^{2-}$) (polymorphs of CaCO_3); (h) $\sim 470 \text{ cm}^{-1}$ and $\sim 1100 \text{ cm}^{-1}$: Si–O–Si bending vibration and Si–O asymmetric stretching (SiO_2 (α -quartz)); (i) $\sim 1795 \text{ cm}^{-1}$ and $\sim 2370 \text{ cm}^{-1}$: C=O (CO_3^{2-} of calcite) and O–C–O (atmospheric CO_2 attack to cement dusts) stretching vibrations; (j) $\sim 2520 \text{ cm}^{-1}$ and $\sim 2880 \text{ cm}^{-1}$: combinational ($\nu_3 + \nu_4$) and $2\nu_3 \text{CO}_3^{2-}$ vibration modes (CaCO_3 polymorphs); (k) $\sim 3412 \text{ cm}^{-1}$: O–H and H–O–H asymmetric stretching vibrations (hydrous portlandite and crystal waters of calcite and gypsum); (l) $\sim 3850 \text{ cm}^{-1}$, $\sim 3645 \text{ cm}^{-1}$, and $\sim 3430 \text{ cm}^{-1}$: C–H bond vibrations (the impure natural/non-natural pozzolanic precursor of the organic traces), O–H stretching (portlandite), and ($\nu_1 + \nu_3$) H_2O combinational vibrations (molecular level water adsorbed/absorbed on/in the surface of the cement particulates), and H-bound OH (H–OH) segments.

All those instrumental inspections and characterizations of the most predominant (alite, belite, and silicates), premier (portlandite and calcite), subsidiary (fly ash, gypsum, aragonite, and vaterite), and ultra-trace (silica, arsenate, and organic traces) level crystallite phases held into the granular cores of Nepal made AP1, AP2, AP3, and AP4 PPC cement brands in dissimilar quantitative proportions not only vowed to assure their quality of NS code and to urge the products monitoring authorities for its timely improvisations on the periphery of the globally modernized clinker formulations of the PPC but also to rate their unequal

performances towards delivering pozzolana specific reaction products, offering good heat of hydration with higher hydration index (HI), enhancing compressive strength, controlling stability of the C–S–H (I) and C–S–H (II) gluing gels, gaining rapid hardening potentialities with better strength index (SI), dispensing stronger binding effects with extremely low risks of water penetration, permeability, absorption, and leakage, providing significant sustainability to the concrete structures with substantial decrement in hair cracking, passivating the reinforced iron bars/rods/sheets/wires, etc. Therefore, this sort of quality assurance study on PPC brands definitely serves as the doctrine means of justifying their explicit founding chemical phases which would be an obvious evidence for branding their products nationwide with reputable public trusts.

ACKNOWLEDGEMENT

The authors are indebted to Nepal Academy of Science and Technology (NAST) for providing the FTIR and XRD measurement facilities. They are thankful to Dr. Rajendra Kumar Pokhrel (Principal, & Assoc. Prof.), Kathford International College of Engineering and Management for the prompt acceptance of this project. The Engineering Chemistry and Applied Science Research Unit of the same institution is acknowledged for bearing the publication cost of this article.

DECLARATION OF AI USAGE

Authors have declared that no any AI tools and the texts generated by them are used.

COMPETING INTERESTS

Authors have declared that no competing interests exist.

REFERENCES

1. (a) P. K. Mehta, P. J. Monteiro, *Concrete: Microstructure, Properties, and Materials* (McGraw-Hill Education; 2013).
(b) S. Thakuri, S. B. Khatri, S. Thapa, *Environ. Sc. Poll. Res.*, 28, 6762(2021).
2. S. Mindess, J. F. Young, D. Darwin, *Concrete* (Prentice-Hall, Upper Saddle River; 2003).
3. S. H. Kosmatka, B. Kerkhoff, W. C. Panarese, *Design and Control of Concrete Mixtures* (5420 Old Orchard Road Skokie, Illinois; 2008).
4. A. M. Neville, *Properties of Concrete* (Pearson Education; 2011).
5. N. N. Kencanawati¹, S. Rawiana¹, N. P. R. Darmayanti, *Aceh Int. J. Sci. Tech.*, 9(1), 40 (2020).
6. A. Jayaswal, *Int. Res. J. Mod. Eng. Tech. Sci.*, 3(3), 871(2021).
7. R. Kumar, Nepal struggles to balance nature and industry, *Nepali Times*, 2022 (Available: <https://nepalitimes.com/banner/nepal-struggles-to-balance-nature-and-industry>)
8. (a) K. Prasain, Nepal will require 26 million tonnes of cement annually by 2024-25, *The Kathmandu Post*, 2021 (Available: <https://kathmandupost.com/money/2021/05/21/nepal-will-require-26-million-tonnes-of-cement-annually-by-2024-25-report->

says#:~:text=Krishana%20Prasain&text=Nepal%20is%20estimated%20to%20require,Rastra%20Bank%20on%20Friday%20showed).

(b) Nepal become self-reliant in clinker, *Khabarhub*, 2019 (Available: <https://english.khabarhub.com/2019/09/53872/>).

9. Top 12 Nepali Cement Brands 2024, 2024 (Available: <https://insightsnp.com/top-12-nepali-cement-brands-2023/>).

10. (a) Nepal cement worth 170 million exported, *Rastrita Samachar Samiti*, 2023 (Available:<https://nepalnews.com/s/business/nepal-cement-worth-170-million-exported#:~:text=Two%20Nepali%20cement%20industries%20have,cement%20since%20October%2017%2C%202022>).

(b) D. Paudel, Increase in cement exports raises hope in Nepal's foreign trade, *Myrepublica Nagariknews*, 2024 (Available: <https://myrepublica.nagariknetwork.com/news/increase-in-cement-exports-raises-hope-in-nepal-s-foreign-trade/>)

(c) Nepal (Imports and Exports), Trade Economy (Available: <https://trendeconomy.com/data/h2/Nepal/6810>).

11. P. R. Pandey, N. Banskota, *Bul. Dep. Geol. Trib. Univ.*, 11, 71(2000).

12. P. Banstola, K. K. Shrestha, I. Thapa, A. K. Mishra, *Int. J. App. Eng. and Management. Lett.*, 5(2), 26(2021).

13. G. Baral, A. B. Marahatta, *Asian J. Appl. Chem. Res.*, 14(4), 34(2023).

14. Department of Geology and Mines, Nepal. Feasibility of clays in Nepal for use in Limestone Calcined Clay Cement (LC). (Available: <chrome-extension://efaidnbmninnibpcapjcgclclefindmkaj/https://www.tara.in/assets/pdf/blue-white-modern-profesional-business-flyer.pdf>)

15. A. B. Marahatta, G. Baral, K. Dhital, *Int. J. Prog. Sci. Tech.*, 45(2), 1(2024).

16. D. Roy, S. K. Sethy, *Int. J. Eng. Res. Sci.*, 3(4), 59(2017).

17. R. Maskey, Energy Use in Nepalese Cement Industries: Case of Udayapur Cement Industries Limited, 2016 (Available: <https://www.academia.edu/68371430>)

18. J. I. Langford, J. C. Wilson, *J. App. Cryst.*, 11, 102(1978).

19. D. M. Smilgies, *J. App. Cryst.*, 42, 1030(2009).

20. R. L. Amhudo, T. T. Raka, I. G. Putu, *Civil Eng. Journal*, 4(8), 1760(2018).

21. C. Mounira, *Journal of Cement Based Composites*, 1, 7(2021).

22. M. Berra, T. Mangialardi, A. E. Paolini, *Adv. Mat. Sci. Eng.* 4853141, 1(2018).

23. A. Singh, S. Gupta, J. Singh, N.P Singh, *Int. J. Res. Eng. Tech.*, 4(5), 60(2015).
24. R. Vedalakshmia, A. Sundara Rajb, S. Srinivasana, K. G. Babu, *Thermochimica Acta* 407, 49(2003).
25. P. A. V. Meulen, E. R. V. Leeuwen, *J. Agri. Res.*, 35(4), 1927.
26. F. P. Glasser, *Mat. Sc. Conc. Calcium Hydroxide in Concrete*, 11 (2001).
27. Y. Lv, J. Qiao, W. Han, B. Pan, X. Jin, H. Peng, *Materials*, 16(6), 2305(2023).
28. R. Agarwal, N. Agnihotri, U. S. Vidyarthi, *J. Eng. App. Sc.*, 8(3), 1(2021).
29. Z. Liu, X. N. Li, D. Deng, G. D. Schutter, L. Hou. *Construction and Building Materials*, 123, 127(2016).
30. T. Staněk, P. Sulovský, M. Boháč, *Cement and Concrete Research*, 92, 21(2017).
31. MIT Concrete Sustainability Hub, Concrete Science Platform White Paper. Improving Concrete Sustainability through Alite and Belite Reactivity (2013). (Available: <chrome-extension://efaidnbmnnnibpcajpcglclefindmkaj/https://cshub.mit.edu/sites/default/files/documents/alite-belite-whitepaper.pdf>)
32. S. Sadeghpour, A. Najafizadeh, A. Kermanpur, *Science & Engineering A*, 584, 177(2013).
33. S. Kumar, V. D. Mote, R. Prakash, V. Kumar, *Materials Focus*, 5, 545(2016).
34. P. B. Belavi, G. N. Chavan, L. R. Naik, V. L. Mathe, R. K. Kotnala, *Int. J. Scient. Tech. Res.*, 2(12), 298(2013).
35. S. Shim, T. Lee, S. Yang, N. Noor, J. Kim, *Materials (Basel)*, 14(16), 4663(2021).
36. M. Y. A. Mollah, M. Kesmez, D. L. Cocke, *Sci. Tot. Env.*, 325, 255(2004).
37. M. Y. A. Mollah, F. Lu, D. L. Cocke, *Sci. Tot. Env.*, 224, 57(1998).
38. National Research Council, National Academy of Sciences, National Academy of Engineering. *Guide to compounds of interest in cement and concrete research*, 1972 (pp. 1-63) (Available: <https://onlinepubs.trb.org/Onlinepubs/sr/sr127.pdf>)
39. L. Badurina, B. Segvic, O. Mandic, G. Zanoni, *Minerals*, 10(10), 899(2020).
40. M. Shiraishi, M. Inagaki, *Carbon Alloys*, 161(2003).
41. P. Głuchowski, R. Tomala, D. Kujawa, V. Boiko, T. Murauskas, P. Solarz, *J. Phys. Chem. C*, 126(16), 7127(2022).